# A STUDY OF MOLECULAR AND LATTICE DYNAMIC OF $Ca(OH)_2$ AND $Ca(OD)_2$ BY INFRARED ABSORPTION AND RAMAN SCATTERING TECHNIQUES

By T. Stanek and G. Pytasz

Department of Chemical Physics, Institute of Chemistry, Jagellonian University, Cracow*

*(Received Nowember 16, 1976)*

Presented here are optical spectra of $Ca(OH)_2$ and $Ca(OD)_2$ associated with one quasiparticle processes corresponding to the Brillouin zone center and those associated with two-quasiparticle processes in the vicinity of 3600 $cm^{-1}$ of the vibronic band of OH group stretching modes. These spectra were used to acquire information from the entire Brillouin zone. This analysis is to a large extent based on a comparison of spectra obtained from ordinary and deuterated samples. The temperature dependence of phonon satellite occurence accompanying the OH vibronic line in the absorption spectrum of $Ca(OH)_2$ in the infrared region and its dependence on the Boltzman population factor are also examined.

## *1. Introduction*

Structural studies [1] have shown that the structure of $Ca(OH)_2$ is hexagonal (space group $D^3_{3d}$). Figure 1 depicts this structure. The lattice parameters are $a = 3.582$ Å and $c = 4.906$ Å. The calcium atom position is (0, 0, 0), whereas the positions of the oxygen atoms are (1/3, 2/3, 0.234) and (2/3, 2/3, −0.234), and those of the hydrogen atoms are (1/3, 2/3, 0.425) and (2/3, 4/3, −0,425). The unit cell contains one molecule. In each unit

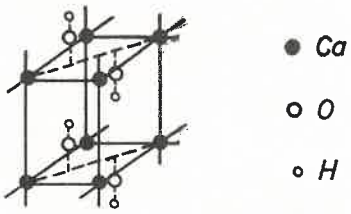


Fig. 1. The crystal structure of $Ca(OH)_2$

* Address: Zakład Fizyki Chemicznej, Uniwersytet Jagielloński Krupnicza 41, 30-060 Kraków, Poland.

TABLE I

The normal modes in the $Ca(OH)_2$

| Class | $N_i$ | $T'$ | $T$ | $R$ | $N_i'$ |
|---|---|---|---|---|---|
| $A_{1g}$ | 2 | 0 | 1 | 0 | 1 |
| $A_{1u}$ | 0 | 0 | 0 | 0 | 0 |
| $A_{2g}$ | 0 | 0 | 0 | 0 | 0 |
| $A_{2u}$ | 3 | 1 | 1 | 0 | 1 |
| $E_g$ | 2 | 0 | 1 | 1 | 0 |
| $E_u$ | 3 | 1 | 1 | 1 | 0 |

Notation: $N_i$ — total number of modes; $T'$ — acoustic translational modes; $T$ — optical translational modes; $R$ — optical rotational modes; $N_i'$ — internal modes of OH group.

TABLE II

A comparison of frequency lattice vibrations in $cm^{-1}$ obtained from infrared spectra of $Ca(OH)_2$, in various works

| R. A. Buchanan et al. [6] | O. Oehler et al. [4] | P. Lagarde et al. [8] | P. Dawson et al. [7] | This paper |
|---|---|---|---|---|
| | 302 $A_{2u}$ | | 288 $E_u(T)$ | 299 Transitional vibration of the type $E_u(T)$ |
| 315 | 321 $E_u$ | 312 $E_u(T)$ | 334 $A_{2u}(T)$ | 401 Rotational vibration of the type $E_u(R)$ |
| 390 | 421 $E_u$ | 345 $A_{2u}(T)$ | 373 $E_u(R)$ | |
| 540 | | 540 $E_u(R)$ | | 543 Translational vibration of the type $A_{2u}(T)$ |

TABLE III

A comparison of frequency lattice vibrations in $cm^{-1}$ obtained from Raman spectra of $Ca(OH)_2$ in various works

| O. Oehler et al. [4] | Z. V. Padanyi [9] | P. Dawson [7] | This paper |
|---|---|---|---|
| 247 $E_g(T)$ | 260 $E_g(T)$ | 254 $E_g(T)$ | 256 Translational vibration of the type $E_g(T)$ |
| 282 $A_{1g}(T)$ | | | |
| 359 $E_g(T)$ | 359 $A_{1g}(T)$ | 357 $A_{1g}(T)$ | 358 Translational vibrational of the type $A_{1g}(T)$ |
| | 684 $E_g(T)$ | 680 $E_g(T)$ | 680 Rotational vibration of the type $E_g(R)$ |

cell there are five atoms, which involves the occurrence of 15 phonon branches. Three of these branches are acoustical, the remaining are optical. Table I presents the division of the normal vibrations in the $Ca(OH)_2$ crystal.

It follows from Table I that the group-theory analysis of the normal vibrations predicts two internal modes of the OH group (stretching modes) associated with bond length changes and possessing $A_{1g}$ and $A_{2u}$ symmetry. Because of the selection rules, the $A_{1g}$ symmetrical mode should show up in the Raman spectrum, and the $A_{2u}$ antisymmetrical mode in the infrared absorption spectrum. In addition, three more lattice vibrations should be expected in the Raman spectra, viz., two translational modes of $A_{1g}$ and $E_g$ symmetry and one rotational mode of $E_g$ symmetry. On the other hand, in the infrared spectrum there should be three peaks linked with two translational lattice vibrations of $A_{2u}$ and $E_u$ symmetry and one rotational vibrations of $E_u$ symmetry.

Examination of the phonon dynamics in the $Ca(OH)_2$ crystal had been done earlier by other authors making use of the infrared absorption method [2–7], Raman spectroscopy [3, 6, 8, 9] and the method of incoherent inelastic neutron scattering [10, 11]. As follows from the comparison of literature data arranged in Tables II and III, there, is a large discrepancy between the various authors regarding both the values of the vibration frequencies and their interpretation. Thus arose the necessity of acquiring our own Raman and infrared spectra, supplemented by the temperature dependence which facilitates the analysis of two-quasiparticle processes.

## *2. Experimental data*

### 2.1. Preparation of $Ca(OH)_2$ and $Ca(OD)_2$ samples

In order to obtain the ordinary calcium hydroxide use was made of the procedure recommended by Detling [12]. In a large crystallizer there were two identical beakers of 100 ml capacity. One had a saturated solution of calcium chloride poured into it, whereas the other had a saturated solution of sodium hydroxide. The crystallizer was then filled carefully with distilled water void of $CO_2$ in such a way that the beakers with their compounds became completely submerged without any occurrence of violent mixing of the liquids. A thin film of paraffin was poured onto the water surface to isolate the whole system from $CO_2$. The crystallizer was placed into a thermostat and maintained at a constant temperature of 30°C for a period of several weeks. The acquired $Ca(OH)_2$ crystals were then rinsed with alcohol and dried.

The deuterated calcium hydroxide $Ca(OD)_2$ was obtained by slaking calcium oxide with heavy water. Red hot CaO was flooded with heavy water $D_2O$ (99%) in the molar ratio of 1 mole CaO per 1 mole $D_2O$. The obtained deuterated calcium hydroxide was dried at 110°C.

### 2.2. Measuring apparatus

Infrared absorption spectra in the lattice vibration range were obtained at room temperature with five spectrometers: two Zeiss spectrometers, types UR-10 and UR-20; a Perkin Elmer spectrometer, type 650; a Grubb Parsons Iris Fourier transform spectro-

meter; and a Digilab Fourier transform spectrometer. The reasons why many instruments were used are as follows. Absorption bands characteristic of the $Ca(OH)_2$ and $Ca(OD)_2$ vibrations lies at the boundary of the far and medium infrared regions. Therefore, the performance of measurements on several spectrometers defined better the data recorded right at the beginning or end of the scale of the used instruments. Moreover, it was interesting to compare the results acquired by the methods of classical spectrometry and Fourier transform spectrometry.

The Raman scattering spectra of $Ca(OH)_2$ and $Ca(OD)_2$, both in range of lattice vibrations and that of the internal vibration of the OH group, were obtained at room temperature with a Varian Cary 82 Raman spectroscope incorporating a laser light source with a 4880 Å exciting line.

## *3. Results and discussion*

### 3.1. Infrared and Raman spectra of $Ca(OH)_2$ and $Ca(OD)_2$ in the range of one-quasi-particle processes

Figures 2, 3 and 4 depict the infrared and Raman spectra of $Ca(OH)_2$ and $Ca(OD)_2$ taken at room temperature in the region of lattice vibrational modes for the purpose of detecting phonon bands corresponding to the Brillouin zone center. In the infrared spectrum of $Ca(OH)_2$, Fig. 2, there are three maxima of the frequencies: 299 $cm^{-1}$, 401 $cm^{-1}$ and 543 $cm^{-1}$. The infrared spectrum of $Ca(OD)_2$, Fig. 3, also features three maxima

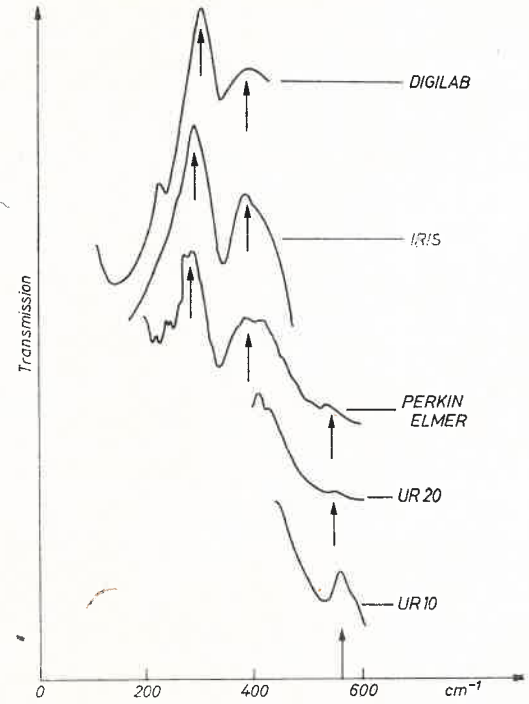


Fig. 2. Infrared absorption spectra of $Ca(OH)_2$

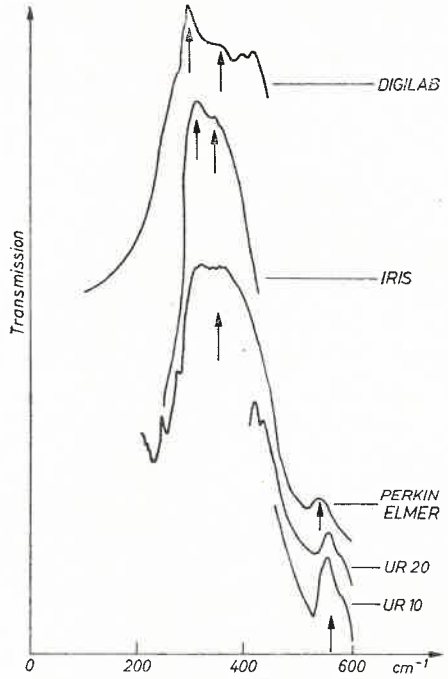


Fig. 3. Infrared absorption spectra of $Ca(OD)_2$

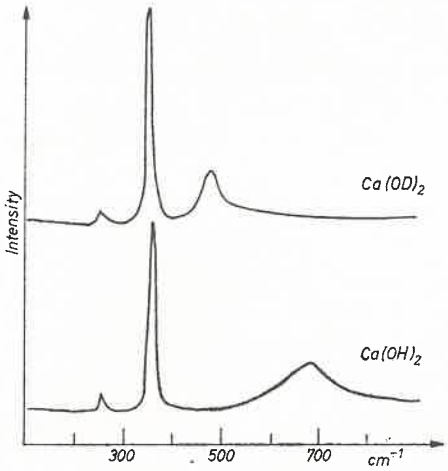


Fig. 4. Raman spectra of $Ca(OH)_2$ and $Ca(OD)_2$

of the frequencies: 307 $cm^{-1}$, 360 $cm^{-1}$ and 546 $cm^{-1}$. These frequencies are mean values of frequencies of the appropriate peaks in the five spectra obtained with the above mentioned five spectrometers.

The Raman spectra of $Ca(OH)_2$ and $Ca(OD)_2$, Fig. 4, feature three maxima in each of the frequencies: for $Ca(OH)_2$ — 256 $cm^{-1}$, 358 $cm^{-1}$ and 680 $cm^{-1}$; and for $Ca(OD)_2$ — 253 $cm^{-1}$, 353 $cm^{-1}$ and 477 $cm^{-1}$.

Group theory analysis shows that in the case of a one quasiparticle process there should be three infrared active absorption bands and three maxima in the Raman spectrum. Of course, group theory does not give a basis for the interpretation of the experimentally obtained bands. This would be facillitated by polarization analysis which could not be applied, however, because powder samples, not single crystals, were examined. Hence, the interpretational guideline was a comparison of the spectra of ordinary and deuterated calcium hydroxide. In both the infrared and Raman spectra the maxima associated with rotational modes ($E_u$ type in the infrared spectrum and $E_g$ type in the Raman spectrum) should become shifted by a factor of $2^{1/2} = 1.42$, whereas the bands of translational vibrational frequencies ($A_{1g}$ and $E_g$ types in the Raman spectrum and $A_{2u}$ and $E_u$ in the infrared spectrum) may only undergo slight changes.

Bearing these facts in mind, the band at the frequency 401 $cm^{-1}$ in the calcium hydroxide's infrared spectrum is interpretated as the band of rotational vibrations of the $E_u$ mode of the OH group; for after deuteration this band shifts to the frequency 360 $cm^{-1}$, though by the factor 1.1 only, much lower than the factor 1.42. On the other hand, the bands at 299 $cm^{-1}$ and 543 $cm^{-1}$ in the case of ordinary calcium hydroxide and 307 $cm^{-1}$ and 546 $cm^{-1}$ in the case of the deuterated substance are interpretated as being of the $E_u$ or $A_{2u}$ mode in which the OH group undergoes translation relative to the metal atom. A confrontation of the frequency of 299 $cm^{-1}$ obtained now with that of 288 $cm^{-1}$ found by Dawson [6] from the infrared reflection spectrum of $Ca(OH)_2$ allows the $E_u(T)$ symmetry to be assigned to the 299 $cm^{-1}$ mode and the $A_{2u}(T)$ symmetry to the 543 $cm^{-1}$ mode.

The Raman spectra in which there are observed three distinct maxima can be interpreted analogously. Two of the peaks, at 256 $cm^{-1}$ and 358 $cm^{-1}$, do not become shifted much after deuteration; hence, they are associated with the translational motions of the OH ion relative to the calcium atom of symmetry $A_{1g}$ and $E_g$. The good agreement of these frequencies with the values obtained by Dawson [6], viz., 254 $cm^{-1}$ and 357 $cm^{-1}$, and with the frequencies obtained by Padanyi [8], viz. 260 $cm^{-1}$ and 357 $cm^{-1}$, from polarized spectra allows the 256 $cm^{-1}$ mode to be interpreted as an $E_g(T)$ translational mode, whereas the 358 $cm^{-1}$ mode as an $A_{1g}(T)$ translational mode. The third peak of a frequency of 680 $cm^{-1}$ in the $Ca(OH)_2$ spectrum becomes shifted after deuteration to 477 $cm^{-1}$, by more or less a factor of $2^{1/2}$, so characteristic of the peak shifts of rotational modes. Taking this into consideration, this peak is interpreted as being a rotational mode maximum of the OH group of $E_g(R)$ symmetry.

The lattice vibration frequencies obtained from absorption spectra in the infrared and Raman scattering spectra in the course of this work are compared with the data of other authors in Tables II and III.

It should be noted that the number of vibrations as found from the optical infrared spectra and Raman spectra in this study agrees with the predictions of group theory. The values of vibration frequencies and their interpretation are generally in agreement with the values and interpretation of the cited authors. Notwithstanding, in some cases there are some essential differences.

### 3.2. Infrared and Raman spectra of $Ca(OH)_2$ and $Ca(OD)_2$ in the range of two-quasi-particle processes

Figures 5 and 6 depict the absorption infrared spectra of $Ca(OH)_2$ nad $Ca(OD)_2$ at room temperature in the range of the OH and OD internal vibrational modes, while Figs 7 and 8 the Raman spectra of these compounds in the same range and temperature. All four spectra possess a complex band structure. The most intense sharp maxima, characterizing the OH stretching mode (the so-called central maxima) at 3645 $cm^{-1}$ in the infrared spectrum (Fig. 5) and 3620 $cm^{-1}$ in the Raman spectrum (Fig. 7) of $Ca(OH)_2$, and those

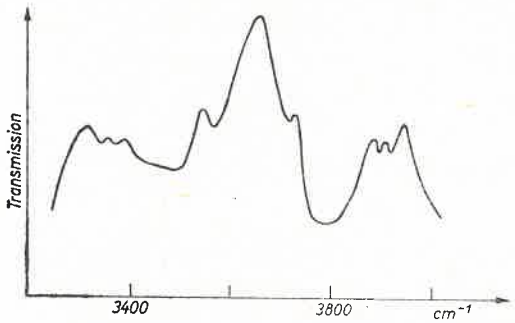


Fig. 5. Infrared absorption spectrum of $Ca(OH)_2$

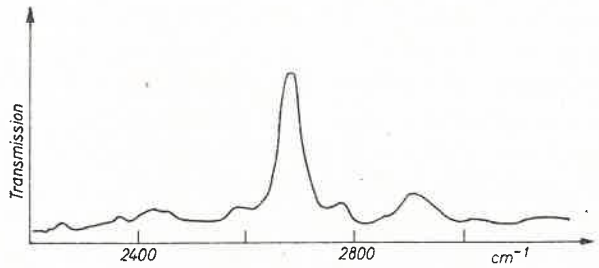


Fig. 6. Infrared absorption spectrum of $Ca(OD)_2$

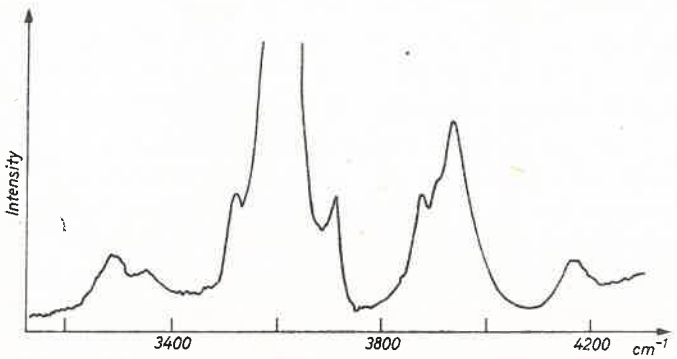


Fig. 7. Raman spectrum of $Ca(OH)_2$

characterizing the OD stretching mode (central maxima) at 2688 $cm^{-1}$ in the infrared spectrum (Fig. 6) and 1662 $cm^{-1}$ in the Raman spectrum (Fig. 8) of $Ca(OD)_2$, are surrounded more or less symmetrically by a series of flanking peaks, the so-called satellites. According to the interpretation of Wickerheim [13], these satellites are the resultant of a combination of OH or OD internal modes with all lattice modes. Hence, the considered

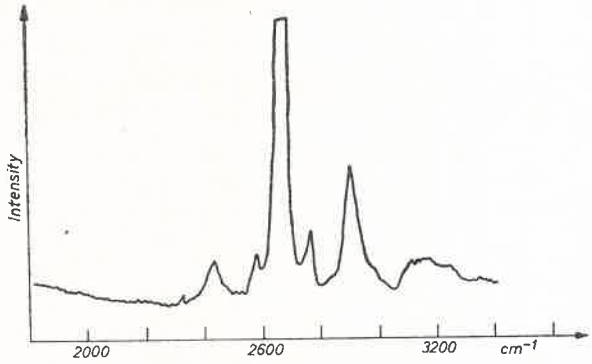


Fig. 8. Raman spectrum of $Ca(OD)_2$

spectral region of the internal modes of the OH and OD groups is associated with the absorption of a photon and simultaneous creation of a vibron along with either the creation or annihilation of a phonon. In the process of photon absorption, therefore, there are involved in this spectral region two quasiparticles: a vibron and a phonon. By calculating the means of the differences between the frequencies of the appropriate maxima on the left and right sides of the central maxima and the frequency of that central peak we get the mean values of the frequencies of hydroxide lattice vibrations. Owing to the combined character of the excitation of an OH vibron $\pm$ lattice phonon or an OD vibron $\pm$ lattice phonon, such events concern to whole Brillouin zone and may therefore be directly compared with the results of neutron studies.

Table IV presents the values of the frequencies of the central maximum and satellites obtained for $Ca(OH)_{12}$ from the infrared and Raman spectra and the calculated differences between the frequencies of the satellites and the central maximum, constituting the frequencies of lattice vibrations of ordinary calcium hydroxide $Ca(OH)_2$. Table V contains similar data for $Ca(OD)_2$ from the infrared and Raman spectra, i.e. the frequencies of the central maxima, satellites and $Ca(OD)_2$ lattice, the latter being calculated as the differences between the frequencies of the satellites and the central maximum.

Table VI gives a comparison of the calculated frequencies of the $Ca(OH)_2$ lattice vibrations of Table IV with the results obtained by the inelastic neutron scattering technique [11]. A comparison of these frequencies allows the mode of the frequency near 100 $cm^{-1}$ to be interpreted as associated with the acoustic phonon branches.

The results obtained by infrared absorption and Raman scattering methods are interpreted accordingly to the suggestion of Wickerheim [13] as evidence of vibron--phonon processes, in which phonons participating in such events originate in the entire

TABLE IV

Frequency of the central line and satellite peaks in $cm^{-1}$ obtained from infrared spectra of $Ca(OH)_2$ and Raman spectra of $Ca(OH)_2$, and frequency lattice vibrations calculated as the difference between satellite peaks and central line frequencies

| The infrared spectroscopy technique | | | | | | The Raman spectroscopy technique | | | | | |
|---|---|---|---|---|---|---|---|---|---|---|---|
| Frequency of satelite peaks at the left side $\nu_1$ | $\nu_{OH}$ | Frequency of satellite peaks at the right side $\nu_2$ | Lattice vibrations | | | Frequency of satellite peaks at the left side $\nu_1$ | $\nu_{OH}$ | Frequency of satellite peaks at the right side $\nu_2$ | Lattice vibrations | | |
| | | | $\frac{\nu_{OH}-\nu_1}{\Delta\nu_1}$ | $\frac{\nu_2-\nu_{OH}}{\Delta\nu_2}$ | $\frac{\Delta\nu_1+\Delta\nu_2}{2}$ | | | | $\frac{\nu_{OH}-\nu_1}{\Delta\nu_1}$ | $\frac{\nu_2-\nu_{OH}}{\Delta\nu_2}$ | $\frac{\Delta\nu_1+\Delta\nu_2}{2}$ |
| 3530 | 3645 | 3730 | 115 | 85 | 100 | 3520 | 3620 | 3720 | 100 | 100 | 100 |
| 3370 | | 3875 | 275 | 230 | 253 | 3350 | | 3875 | 270 | 255 | 263 |
| 3340 | | 3900 | 305 | 255 | 280 | 3300 | | 3930 | 320 | 310 | 315 |
| 3300 | | 3930 | 345 | 285 | 315 | | | | | | |

TABLE V

Frequency of the central line and satellite peaks in $cm^{-1}$ obtained from infrared spectra of $Ca(OD)_2$ and Raman spectra of $Ca(OD)_2$, and frequency lattice vibrations calculated as the difference between satellite peaks and central line frequencies

| The infrared spectroscopy technique | | | | | | The Raman spectroscopy technique | | | | | |
|---|---|---|---|---|---|---|---|---|---|---|---|
| Frequency of satellite peaks at the left side $\nu_1$ | $\nu_{OD}$ | Frequency of satellite peaks at the right side $\nu_2$ | Lattice vibrations | | | Frequency of satellite peaks at the left side $\nu_1$ | $\nu_{OD}$ | Frequence of satellite peaks at the right side $\nu_2$ | Lattice vibrations | | |
| | | | $\frac{\nu_{OD}-\nu_1}{\Delta\nu_1}$ | $\frac{\nu_2-\nu_{OD}}{\Delta\nu_2}$ | $\frac{\Delta\nu_1+\Delta\nu_2}{2}$ | | | | $\frac{\nu_{OD}-\nu_1}{\Delta\nu_1}$ | $\frac{\nu_2-\nu_{OD}}{\Delta\nu_2}$ | $\frac{\Delta\nu_1+\Delta\nu_2}{2}$ |
| 2580 | 2688 | 2770 | 108 | 112 | 110 | 2582 | 2662 | 2756 | 80 | 94 | 87 |
| 2455 | | 2910 | 233 | 222 | 228 | 2437 | | 2894 | 225 | 232 | 229 |
| 2425 | | | 263 | | | | | | | | |
| 2365 | | | 323 | | | | | | | | |
| 2345 | | 3030 | 343 | 342 | 343 | 2325 | | | 337 | | |
| 2265 | | | 423 | | | | | 3112 | | 450 | |
| | | | | | | | | 3150 | | 488 | |
| | | | | | | | | 3216 | | 554 | |

TABLE VI

Comparison of lattice mode frequencies of $Ca(OH)_2$, in $cm^{-1}$

| Infrared method (present study) | Raman method (present study) | Incoherent inelastic neutron scattering method [12] |
|---|---|---|
| 100 | 100 | 100 |
| 253 | 263 | 250 |
| 280 | | 310 |
| 315 | 315 | 340 |
| | | 530—550 |

TABLE VII

Table of characterrs for $D_{3d}$ symmetry group

| Symmetry of vibration | Symmetry elements of $D_{3d}$ group | | | | | | |
|---|---|---|---|---|---|---|---|
| | $E$ | $2C_3$ | $3C_2$ | $i$ | $2S_6$ | 3 | |
| $A_{1g}$ | 1 | 1 | 1 | 1 | 1 | 1 | $x^2+y^2, z^2$ |
| $A_{2g}$ | 1 | 1 | −1 | 1 | 1 | −1 | $R_z$ |
| $E$ | 2 | −1 | 0 | 2 | −1 | 0 | $(R_xR_y)$ $(x^2-y^2, xy)$ $(xz, yz)$ |
| $A_{1u}$ | 1 | 1 | 1 | −1 | −1 | −1 | |
| $A_{2u}$ | 1 | 1 | −1 | −1 | −1 | 1 | $z$ |
| $E$ | 2 | −1 | 0 | −2 | 1 | 0 | $(x, y)$ |

Brillouin zone, and not its center alone. The various satellite maxima should correspond to maxima in the phonon frequency distribution function, that is, to maxima in the phonon state density plot. Hence, optical spectroscopy may be used as a tool for examining phonon spectra.

Since the symmetry of all vibrations is known, the selection rules in two-phonon processes observed by optical spectroscopic methods can be predicted. All lattice vibrational modes of wave vector $q = 0$ are described by one of the irreducible representations of the $D_{3d}$ symmetry group (Table VII).

Multiplication of the representation of the hydroxide group's internal mode by that of the lattice vibration leads to selection rules for the two-phonon process. The OH group vibrational modes of $A_{1g}$ symmetry active in the Raman spectrum in combination with the lattice vibration may give an infrared- or Raman-active mode. Likewise, the OH vibrational mode of $A_{2u}$ symmetry active in the infrared absorption spectrum may give in combination with a phonon an infrared- or Raman-active mode. On the basis of the table of characters for the $D_{3d}$ group (Table VII), we find the representation products of interest, which define the symmetry of two-phonon processes: $A_{1g}\times A_{1g} = A_{1g}$, $A_{1g}\times E_g = E_g$, $A_{1g}\times A_{2u} = A_{2u}$, $A_{1g}\times E_u = E_u$, $A_{2u}\times A_{1g} = A_{2u}$, $A_{2u}\times A_{2u} = A_{1g}$, $A_{2u}\times E_g = E_u$, $A_{2u}\times E_u = E_g$.

As is seen, in the absorption spectrum in the infrared there should be, because of their activity, the following combinational vibrations of the symmetries $A_{1g} \times A_{2u}$, $A_{1g} \times E_u$, $A_{2u} \times A_{1g}$, $A_{2u} \times E_g$.

On the other hand, in the Raman spectrum there should be the vibrations $A_{1g} \times A_{1g}$, $A_{1g} \times E_g$, $A_{2u} \times A_{2u}$, $A_{2u} \times E_u$.

TABLE VIII

Comparison of calculated satellite frequencies with values read from the infrared and Raman spectra of $Ca(OH)_2$, in $cm^{-1}$

| Infrared spectrum | | Raman spectrum | |
|---|---|---|---|
| Calculated | Read | Calculated | Read |
| | | 2940 | |
| 2965 | | 2978 | |
| 3080 | | 3105 | |
| 3219 | | 3249 | |
| 3320 | 3300 | 3262 | |
| 3392 | 3340 | | 3300 |
| | | 3345 | 3350 |
| 3407 | | 3367 | |
| | 3530 | | 3520 |
| | 3720 | | 3720 |
| | 3875 | 3873 | 3875 |
| 3839 | 3900 | 3945 | 3930 |
| 3920 | 3930 | 3978 | |
| 4018 | | 4046 | |
| 4021 | | 4185 | |
| 4160 | | 4300 | |
| 4325 | | | |

Table VIII presents the frequencies calculated thus, which should occur for the satellites in the infrared and Raman spectra, as long as only excitations with $q = 0$ react as phonons, that is, the frequencies obtained from the infrared and Raman spectra concerning one-phonon processes presented earlier. The table also contains for the sake of comparison the experimental frequencies of the satellites read from the infrared absorption spectrum of $Ca(OH)_2$ (Fig. 5) and the Raman spectrum of $Ca(OH)_2$ (Fig. 7). There are rather large discrepancies between the column of calculated values and the column of values obtained from the recording of satellites. It is evident that the satellites should reach far out to both sides of the central maximum both in the infrared abd Raman spectrum. The lacking experimental evidence may perhaps be due to their low intensity. On the other hand, the occurrence of a greater number of satellites in the nearest neighborhood of the central peak than would stem from calculations is proof that the combination model presented here and taking only phonons from the Brillouin zone center into account is too simple. Hence,

phonons from the entire Brillouin zone should be considered together with the acoustic phonons, which would then increase the number of combinations as compared with values calculated in Table VIII.

### 3.3. Investigation of the temperature dependence of satellite occurrence in the infrared spectrum of $Ca(OH)_2$

Figure 9 shows the absorption spectra of $Ca(OH)_2$ in the infrared obtained at the following temperatures: room temperature, 0°C, −50°C, −80°C, −100°C, −130°C, −150°C and −152°C. With the decreasing temperature we observe a change in the structure and intensities of the satellite maxima — different for the difference (vibron−phonon)

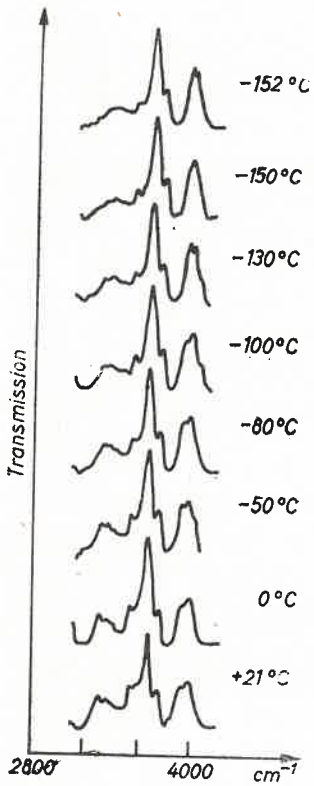


Fig. 9. Infrared absorption spectra of $Ca(OH)_2$ at various temperatures

maxima, and different for the summation (vibron+phonon) maxima. On the left-hand side of the central peak the intensities decrease, whereas on the right-hand side they increase as the temperature drops.

This type of changes can be explained as follows. At low temperature there are few phnons in the sample. Therefore, there are rarely observed processes linked with the annihilation of any existing phonons. But processes linked with phonon creation are observed. Well, the left-hand side of the the satellite band is the side in which a photon

was forced to excite a vibron and simultaneously annihilate a phonon. In view of the low density of phonons in the sample this annihilation cannot occur with a high probability and because of this the left-hand side of the satellite band is of low intensity at low temperatures. The right-hand side of the satellite bands, on the other hand, is associated with simultaneous creation of a vibron and a phonon, and this may occur without restrictions, even at low phonon density in the sample. At high temperature the situation becomes evened out. The creation processes remain almost invariable with respect to the low temperature circumstances, whereas phonon annihilation may now occur almost without any restrictions owing to the large phonon density in the sample at this temperature. Whence the intensities of the two sides of the satellite bands are more or less even at this temperature.

### *4. Conclusions*

Recapitulating, it must be found that the phonon dynamics of calcium hydroxide is characterized by three phonon types, viz. two optical translational and one rotational type, which remains in agreement with group-theory predictions. The frequencies of these phonons determined from the infrared absorption and Raman scattering spectra in the low frequency region allow the phonon bands corresponding to the Brillouin zone center to be found, that is, the bands corresponding to one-quasiparticle events associated with the creation or annihilation of a phonon. Moreover, the calcium hydroxide lattice dynamics features an OH vibron depicted in the infrared and Raman spectra as a sharp peak with phonon satellites on each side. The satellite maxima are interpreted as originating from two-quasiparticle vibron $\pm$ phonon processes, which is compatible with the suggestion of Wickerheim. Thanks to this interpretation of the origin of the satellite peaks information was obtained from optical measurements regarding the density of phonon states in the whole Brillouin zone. This information is comparable and in good agreement with the data obtained by the method of incoherent inelastic neutron scattering.

This interpretation of the origin of the satellites is backed up by their temperature dependence, which is a fine illustration of the mechanism associated with phonon creation and annihilation.

Our thanks are due to Docent J. M. Janik and Professor J. A. Janik for stimulating discussion. The author wish to express their gratitude to Professor B. Trzebiatowska of the Wrocław University for the use of the Perkin Elmer spectrometer, to Professor E. Görlich of the Academy of Mining and Metallurgy in Cracow for the use of the Digilab spectrometer, to Docent R. Konopka of the Silesian University for the use of the UR-20 spectrometer, and to Regional Laboratory of Physical-Chemical Analysis and Structure Research of the Jagellonian University for making measurements on the Raman spectrometer Cary 82 possible.

### REFERENCES

[1] W. R. Busing, H. Levy, *J. Chem. Phys.* **26**, 563 (1957).
[2] R. M. Hexter, *J. Opt. Soc. Amer.* **48**, 770 (1958).
[3] O. Oehler, H. H. Gunthard, *J. Chem. Phys.* **48**, 2036 (1968).

[4] W. R. Busing, H. H. Morgan, *J. Chem. Phys.* **28**, 998 (1958).
[5] R. A. Buchanan, H. H. Caspers, J. Murphy, *Appl. Optics* **2**, 1147 (1963).
[6] P. Dawson, C. D. Hadfield, G. R. Wilkinson, *J. Chem. Phys.* **34**, 1217 (1973).
[7] P. Lagarde, M. A. Nerenberg, Y. Farge, *Phys. Rev.* **B4**, 1731 (1973).
[8] Z. V. Padanyi, *Solid State Commun.* **8**, 541 [1970].
[9] D. Krishnamurti, *Proc. Indian Acad. Sci.* **A50**, 232 (1959).
[10] G. Safford, V. Brajovic, H. Boutin, *J. Phys. Chem. Solids* **24**, 771 (1963).
[11] A. Bajorek, J. A. Janik, J. M. Janik, I. Natkaniec, T. Stanek, T. Wasiutyński, *Acta Phys. Pol.* **A40**, 431 (1971).
[12] W. Conrad, K. D. Detling, *J. Chem. Educ.* **113**, 176 (1934).
[13] K. A. Wicherheim, *J. Chem. Phys.* **31**, 863 (1959).